The McClure Mountain Syenite Apatite as a Potential Age Control Reference Material for LA-ICP-MS AFT and U-Pb Double Dating

Nathan Cogné, Alexis Derycke, Kerry Gallagher

GEOSTANDARDS and GEOANALYTICAL RESEARCH

The McClure Mountain Syenite Apatite as a Potential Age Control Reference Material for LA-ICP-MS AFT and U-Pb Double Dating

Nathan **Cogné** (1)*, Alexis **Derycke** (2) and Kerry **Gallagher** (1)

(1) Géosciences Rennes, UMR6118, CNRS Université de Rennes, France
(2) Université de Lorraine, CNRS, CRPG, F-54000 Nancy, France
* Corresponding author. e-mail: nathan.cogne@univ-rennes.fr

Apatite fission track (AFT) dating is now routinely performed using LA-ICP-MS, and U-Pb age data are often acquired at the same time, allowing double dating of individual grains. Furthermore, additional geochemical data, such as REE mass fractions are readily acquired during the analysis. It is therefore of practical interest to identify a single material as a quality control on ages and composition. Here we present AFT and U-Pb data for the McClure Mountain Syenite (MMS) apatite, already widely used as an age reference material by the U-Pb community. We performed double dating on 238 grains, in thirteen measurement sessions over two years. The AFT data show remarkable reproducibility with an overall central age of 254.1 ± 5.1 Ma. The U-Pb results agree with the reference age for individual sessions (and for all data together). The results show that that the McClure Mountain apatite is a valid quality control material for double dating, allowing the use of the same material for both methods. We also propose to extend the quality control using MMS to trace element measurements performed in conjunction AFT and U-Pb dating.

Keywords: AFT and U-Pb double dating, LA-ICP-MS, apatite, reference material, McClure Mountain syenite.

Received 01 Dec 23 – Accepted 25 Jan 24

The fission track dating method, based on the counting of the linear defects created by spontaneous fission of ^{238}U in apatite, zircon and some other minerals, was developed during the 1960s and 1970s (e.g., Price and Walker 1962, Fleischer *et al.* 1975). Various techniques were considered for uranium content measurement before settling on the external detector method with a ζ empirical calibration (EDM, Hurford and Green 1983, Hurford *et al.* 1990). The method requires sample irradiation by thermal neutrons to produce artificial or induced ^{235}U tracks (to estimate the ^{238}U content via the known isotopic ratio). The ζ calibration relies on well-calibrated age reference materials that are widely available and homogeneous in age, such as Durango (e.g., McDowell *et al.* 2006) and Fish Canyon (e.g., Boehneke and Harrison 2014). The calibration factor is obtained for each analyst individually and is regularly monitored by recounting old and new reference materials. Therefore, using the EDM method, the FT community rarely report secondary reference material calibrations alongside published datasets. We define a secondary reference material or quality control reference material as an internationally recognised sample of known age treated as an unknown, while a primary age reference material is a sample of known age against which all measurements can be calibrated.

For various reasons, not least the logistics involved in irradiation, the use of laser ablation-inductively coupled plasma-mass spectrometry (LA-ICP-MS) for determination of U content has been developed over the last 15–20 years and is now widely used, mainly for apatite. Two different approaches are used for U measurement: (i) an absolute approach (e.g., Hasebe *et al.* 2004, De Grave *et al.* 2012, Soares *et al.* 2014), and (ii) a modified ζ method (e.g., Donelick *et al.* 2005, Chew and Donelick 2012, Cogné *et al.* 2020). In parallel, statistical tools for processing the

doi: 10.1111/ggr.12545

data (such as handling zero spontaneous track grains, mixture modelling, radial plots) have also been developed (Galbraith 2010, Vermeesch 2017, 2019). The use of a secondary reference material to test the accuracy of the data reduction scheme with 'standard' bracketing and the reporting of this secondary reference material data is common practice for other laser ablation geochronology communities using LA-ICP-MS (e.g., Horstwood *et al.* 2016 for U-Pb or Glorie *et al.* 2023 for Rb-Sr). Although the FT dating community often uses an in-house apatite age reference material, the data are rarely published.

Given this, we argue that using a secondary reference material is important for the FT community as it ensures that the quality of both counting and data processing can be assessed *a posteriori*. Furthermore, as the LA-ICP-MS method allows for acquisition of other data (often U-Pb dating and trace element mass fractions) on the same laser spot used for U determination (e.g., Chew and Donelick 2012, Chew *et al.* 2016), it is of practical interest that the secondary reference material used for FT dating should be used in similar way for U-Pb dating and/or trace element mass fractions. Quality control can then be performed on the same ablation spot for the different methods.

Currently, there are apatite reference materials distributed among the FT community, mainly Durango and Fish Canyon. However, these two reference materials are both relatively young, which creates two drawbacks. First, spontaneous tracks need to be counted over a large area to reach a sufficient number of tracks to constrain the age to an appropriate precision. This in turn implies the analysis of a large number of areas with LA-ICP-MS, increasing the analysis time. Second, young samples are not particularly useful as U-Pb dating reference materials. Iwano *et al.* (2019) proposed the Duluth Complex apatite as an FT reference material for LA-ICP-MS dating. However, while this reference material is well known for zircon U-Pb dating, to date it is not widely distributed, nor characterised for apatite U-Pb dating. LA-ICP-MS apatite U-Pb dating yields a slightly younger age than zircon U-Pb (1078 ± 12 Ma for apatite, Härtel *et al.* 2023, compared with 1099.0 ± 0.6 Ma for zircon, Paces and Miller 1993) but no TIMS characterisation exists. This characterisation is important to constrain both the reference age and the common Pb isotopic composition, the latter being used to anchor the discordia in Tera-Wasserburg diagrams, thereby increasing the precision of the estimated age. Also, the FT apatite age is relatively old (*ca.* 850–900 Ma, Iwano *et al.* 2019, Cogné and Gallagher 2021) compared with most published apatite FT ages, so is relatively atypical.

In contrast, the McClure Mountain Syenite Complex (MMS) apatite is often used as a primary or secondary reference material for U-Pb dating (e.g., Chew *et al.* 2014a) and is characterised by TIMS (Schoene and Bowring 2006, Krestianinov *et al.* 2021). Therefore, this presents a possible double dating reference material for both U-Pb and FT dating of apatite. Here, we present FT, U-Pb and trace element data acquired over the past two years on the MMS apatite and propose it as a secondary reference material for apatite FT and U-Pb double dating. Additionally, we compare our trace element data with a large LA-ICP-MS trace element dataset previously published (Chew *et al.* 2016) and suggest that the MMS could also be used as secondary reference material for trace element mass fractions. In that context, we do not address the geological/thermal history of the MMS here, our aim being only to assess its use as a new control reference material.

McClure Mountain Syenite (MMS) Complex

The MMS complex outcrop spans an area of approximately 46 km^2 in the northern Wet Mountains (Colorado, USA) (Olson *et al.* 1977). The complex was intruded in Precambrian metamorphic basement and is composed of mafic-ultramafic layered intrusions that are themselves intruded by hornblende-biotite syenite and nepheline syenite (Shawe and Parker 1967). The major constituents of the hornblende-biotite syenite are K-feldspar, plagioclase, hornblende, biotite and pyroxene, while titanite and apatite make up several percent of the rock (Schoene and Bowring 2006). Zircon, baddeleyite, calcite, nepheline, magnetite, ilmenite, zirconolite and alteration products are minor constituents, making up < 2% of the rock (Schoene and Bowring 2006).

Numerous geochronological studies have been published on the MMS (Table 1). The MMhb K/Ar hornblende reference material was extracted from MMS and has been dated at 519.5 ± 5.0 Ma (Alexander *et al.* 1978, here, and throughout this publication, uncertainties are quoted at the 2*s* level) and at 520.4 ± 3.4 Ma by interlaboratory cross calibration (Samson and Alexander 1987). Subsequently, Spell and McDougall (2003) provided a total fusion $^{40}Ar/^{39}Ar$ date of 523.3 ± 1.8 Ma. Schoene and Bowring (2006) published an isotope dilution, thermal ionisation mass spectrometry (ID-TIMS) $^{207}Pb/^{235}U$ zircon date of 523.98 ± 0.12 Ma interpreted as the crystallisation age. In the same publication they also provided titanite and apatite weighted mean $^{207}Pb/^{235}U$ ages at 523.26 ± 0.65 Ma and 523.51 ± 1.47 Ma respectively. Common lead compositions were also reported in the same contribution

Table 1.
Summary table of previously published geochronology data on the McClure Mountain syenite (MMS)

Reference	Method used	Mineral	Age range or age (Ma)
Olson *et al.* (1977)	Fission Track	Apatite	239 ± 52
Olson *et al.* (1977)	Fission Track	Titanite	506 ± 43
Alexander *et al.* (1978)	K/Ar	Hornblende	519.5 ± 5
Samson and Alexander (1987)	K/Ar	Hornblende	520.4 ± 3.4
Spell and McDougall (2003)	Ar-Ar	Hornblende	523.3 ± 1.8
Schoene and Bowring (2006)	U-Pb	Zircon	523.98 ± 0.12
Schoene and Bowring (2006)	U-Pb	Titanite	523.26 ± 0.65
Schoene and Bowring (2006)	U-Pb	Apatite	523.51 ± 1.47
Krestianinov *et al.* (2021)	U-Pb	Apatite	525.3 ± 1.7
Anderson *et al.* (2017)	U-Th-Sm/He	Zircon	474–230.3
Anderson *et al.* (2017)	U-Th-Sm/He	Titanite	523–447
Anderson *et al.* (2017)	U-Th-Sm/He	Apatite	138.9–88
Weisberg *et al.* (2018)	U-Th-Sm/He	Zircon	567–381
Weisberg *et al.* (2018)	U-Th-Sm/He	Titanite	501–488
Weisberg *et al.* (2018)	U-Th-Sm/He	Apatite	211–70

at $^{206}Pb/^{204}Pb$ = 17.54 ± 0.27 and $^{207}Pb/^{204}Pb$ = 15.47 ± 0.04 for apatite. More recently, Krestianinov *et al.* (2021) produced TIMS data on apatite, obtaining a 3D isochron age of 525.3 ± 1.7 Ma, which is in agreement with the age of Schoene and Bowring (2006). Using their data and those of Schoene and Bowring (2006) they proposed new common lead compositions of $^{206}Pb/^{204}Pb$ = 17.78 ± 0.18 and $^{207}Pb/^{204}Pb$ = 15.539 ± 0.038 for apatite, that are also in agreement with the previously reported values.

Olson *et al.* (1977) produced a titanite FT age of 506 ± 43 Ma. More recently a large dataset of (U-Th)/He dates was published on titanite, zircon and apatite (Anderson *et al.* 2017, Weisberg *et al.* 2018). Quoting only data that probably come from the same area as the original aliquot (MM1 sample) of Alexander *et al.* (1978), the ages range from 447 ± 12 to 523 ± 14 Ma for titanite, 230.3 ± 7.7 to 480 ± 9 Ma for zircons and 70 ± 2 to 150 ± 9 Ma for apatite (note the apatite and zircon ages are alpha ejection, or Ft, corrected).

Only one FT apatite age has been published on the MMS (Olsen *et al.* 1977) using the protocol outlined by Naeser (1967). Updating the spontaneous decay constant (λ_f) from the original value of 6.85×10^{-17} to the now accepted value of 8.45×10^{-17} (Holden and Hoffman 2000 would change the originally published age of 293 ± 62 Ma to 239 ± 52 Ma, although it is likely that other unknown calibration errors were also involved, making this simple recalculation unreliable. In any case, this AFT age is largely uncertain. Kelley and Chaplin (2004) reported a large number of fission track ages in the Wet Mountains. Close to the vicinity of MMS, and at similar elevation (approximately 2300 m), the FT ages range from 141 ± 10 Ma to 299 ± 20 Ma. Overall, the available geochronological data imply an expected apatite FT age between 200 and 300 Ma.

Sample and methods

To characterise MMS we used apatite separates from sample MM1, which was kindly provided by Ray Donelick. MM1 comes from "a boulder from the parking lot" (Donelick, pers. comm.) and aliquots from this same locality have been widely distributed to laboratories by Ray Donelick and Trinity College Dublin. It is likely to be from the same sample as sample MM1 of Weisberg *et al.* (2018) and from the same location than that described by Anderson *et al.* (2017). Apatites from this separate are euhedral and usually between 50 and 250 µm diameter. In cathodoluminescence (CL) they show a weak concentric to negligible zonation (Figure 1a), similar to that reported by Schoene and Bowring (2006).

Over two years thirteen measurement sessions were performed involving double FT and U-Pb dating of 240 crystals, on three different mounts (see Table 2). The first 130 grains, on the first mount, were also measured for trace elements (Mn, Sr, Y, REE). All mounts were 1.5 mm thick epoxy discs of 2 cm diameter. For FT dating, we followed the ζ protocol of Cogné *et al.* (2020). Firstly, large (a few thousands of mm^2) areas were delimited for counting a large number of tracks. Then a first "primary" session was performed to characterise each area in terms of the U/Ca ratio and to calculate a precise ζ factor. Because Durango is quite homogeneous in U (apart from the outer rims), the analysed large area could subsequently be revisited during measurement sessions on unknowns to establish a fractionation factor, allowing the use of the primary ζ for age calculation.

Track etching was performed with 5.5 mol l^{-1} HNO_3 at 21 °C for 20 s. The grain mounting and etching are similar to the protocol described by Donelick *et al.* (2005). Spontaneous fission track counting was carried out using a Zeiss Axio Imager M1 equipped with an automated stage

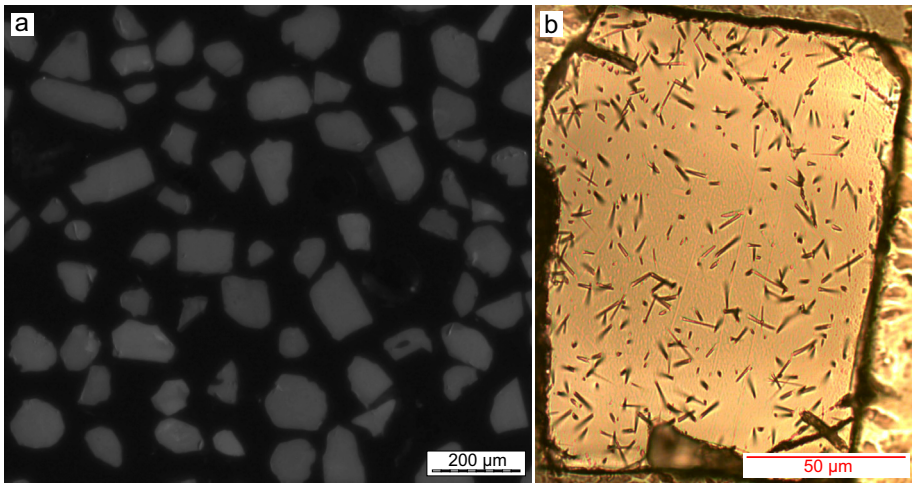

Figure 1. (a) CL image of MM-1 apatite separate. Very weak concentric zoning to no pattern is visible. (b) Typical MM-1 grain after etching. The track density allows potential U zoning to be seen while also allowing the grain to be easily counted.

Table 2.
Summary table of measurement results for FT and U-Pb dating

Session	Mount / type of analyses	Ablation pattern	*N* grains	*Ns*	ρ_s (track cm^{-2})	U/Ca mean	AFT central age (Ma)	2*s* (Ma)	*p*(χ^2)	Dispersion (%)	U-Pb age (Ma)	2*s* (Ma)	MSWD
Session 1	1 / AFT+UPb+ REE	30 µm round; 5 Hz; 3.9 J cm^{-2}	40	1669	1.88E+06	5.32E-03	252.1	12.6	0.54	0.0	527.2	7.1	0.34
Session 2	1 / AFT+UPb+ REE	30 µm round; 5 Hz; 3.9 J cm^{-2}	20	664	1.71E+06	4.58E-03	269.2	22.1	0.35	4.8	530.0	9.6	0.45
Session 3	1 / AFT+UPb+ REE	30 µm round; 5 Hz; 3.9 J cm^{-2}	10	336	1.57E+06	4.27E-03	269.6	37.1	0.16	11.1	527.2	13.0	0.34
Session 4	1 / AFT+UPb+ REE	30 µm round; 5 Hz; 3.9 J cm^{-2}	8	266	2.02E+06	5.19E-03	281.6	35.2	0.87	0.0	531.6	13.8	1.33
Session 5	1 / AFT+UPb+ REE	30 µm round; 5 Hz; 3.9 J cm^{-2}	9	232	1.41E+06	3.61E-03	271.4	36.0	0.99	0.0	528.0	12.8	1.38
Session 6	1 / AFT+UPb+ REE	30 µm round; 5 Hz; 3.9 J cm^{-2}	13	420	2.05E+06	5.68E-03	253.0	25.4	0.76	0.0	522.8	7.9	0.98
Session 7	1 / AFT+UPb+ REE	30 µm round; 5 Hz; 3.9 J cm^{-2}	10	299	1.65E+06	4.52E-03	279.8	33.1	0.82	0.0	518.9	8.2	0.53
Session 8	1 / AFT+UPb+ REE	30 µm round; 5 Hz; 3.9 J cm^{-2}	20	626	1.86E+06	5.05E-03	255.1	20.9	0.51	0.0	522.5	6.8	0.46
Session 9	2 / AFT +UPb	10*10 µm raster 60 Hz 20 µm s^{-1}	20	3597	1.30E+06	3.61E-03	251.8	11.7	0.12	5.1	511.5	7.4	1.00
Session 10	2 / AFT +UPb	40*40 µm square; 5 Hz; 3.9 J cm^{-2}	14	564	1.42E+06	4.22E-03	245.6	24.6	0.17	9.5	523.3	4.9	0.66
Session 11	2 / AFT +UPb	40*40 µm square; 5 Hz; 3.9 J cm^{-2}	25	1139	1.36E+06	4.20E-03	238.4	15.1	0.32	4.8	525.1	4.3	1.04
Session 12	2 / AFT +UPb	40*40 µm square; 5 Hz; 3.9 J cm^{-2}	19	1048	1.53E+06	4.46E-03	240.2	16.6	0.27	6.0	519.9	4.1	1.02
Session 13	3 / AFT +UPb	40*40 µm square; 5 Hz; 3.9 J cm^{-2}	30	1728	2.02E+06	5.50E-03	261.1	12.9	0.33	0.0	527.3	4.2	0.79

Ns, Number of counted spontaneous tracks.

system using TrackWorks software at a magnification of 1000×. This software was used when measuring a total of 196 confined track lengths and their angle to the *c* axis, as well as Dpar, on seventy grains (forty on mount 1, 30 on mount 3). Only sub-horizontal tracks in track (TINTS) were measured.

All laser ablations, apart for session 9 (see below), were performed at the University of Rennes GeOHeLiS analytical platform, using an ESI NWR193UC Excimer laser coupled to an Agilent 7700x Q-ICP-MS. We employed an energy of 3.9 J cm^{-2} and a repetition rate of 5 Hz. Sessions 1 to 8 used a round 30 μm spot, while sessions 10 to 13 used a 40 × 40 μm square. One grain was destroyed during laser ablation in both sessions 10 and 11. Session 9 was performed in Trinity College Dublin, using a mapping approach (see Ansberque *et al.* 2020 for details) on a Photon Machines Iridia 193 nm ArF excimer laser-ablation system coupled to an Agilent 7900 Q-ICP-MS. The mapping was performed with raster of 10 μm × 10 μm squares over each grain. The scanning speed was set up at 20 μm s^{-1}, with energy of 2 J cm^{-2} and a repetition rate of 60 Hz. As the mapping allows counting tracks over a larger area, because the whole grain is analysed by LA-ICP-MS, it produces more precise single grain and central ages.

For sessions 1 and 13 the MM1 grains were ablated as an unknown, i.e., fifteen to twenty grains in a row between two series of reference materials. A series of reference material is the suite of three analyses on NIST SRM 612 glass (Jochum *et al.* 2011), three analyses on Madagascar apatite (U-Pb primary reference material, Thomson *et al.* 2012), and three analyses on Durango Zeta apatite (see Cogné *et al.* 2020). One mapping session (session 9) was dedicated to MM1 dating and three grains were analysed between each batch of reference materials (same as above, except that instead of spots, the reference materials were ablated with a rastered mapping approach). For the remainder of the sessions, MM1 grains were positioned in the reference material batch, with two or three grains in a row either side of a batch of approximately twenty unknowns. For each session the number of analysed MMS grains was between eight and forty. LA-ICP-MS data were processed using Iolite software v4 (Paton *et al.* 2011), using Trace Elements DRS (Woodhead *et al.* 2007) for trace element mass fraction, a modified version of it (Cogné *et al.* 2020) for FT dating and VizualAge_UComPbine DRS (Chew *et al.* 2014a) for U-Pb dating. Chlorine content was also measured using the protocol of Chew *et al.* (2014b) and a synthetic Cl-apatite (Klemme *et al.* 2013) as high-Cl reference material.

The FT dating used the ζ protocol of Cogné *et al.* (2020). Artificial glass NIST SRM 612 (Jochum *et al.* 2011) was used to correct machine drift and Durango apatite shards analysed during a primary session were revisited to calculate the fractionation factor. The age calculation was implemented in an in-house python script and produced single grain ages as well as both central and pooled ages, $p(\chi^2)$, and dispersion for the dated sample. Trace element estimations were made using NIST SRM 612 as the calibration reference material and ^{43}Ca as the internal standard element. The chondrite values used to normalise trace element mass fractions are from Barrat *et al.* (2012). The Madagascar apatite (Thomson *et al.* 2012) was used as the primary reference material to calculate U-Pb ratios. An in-house python script was used for U-Pb age calculation. The York *et al.* (2004) algorithm was used to calculate the best-fit regression line (and its uncertainty envelope) for the population of $^{207}Pb/^{206}Pb$ and $^{238}U/^{206}Pb$ ratios. The lower intercept of this line with the Concordia in the Tera-Wasserburg space (and its uncertainty) was calculated using the approach of Ludwig (1980). The *y* intercept of the best-fit line was anchored to a $^{207}Pb/^{206}Pb$ value of 0.874 (Krestianinov *et al.* 2021).

Results

All results are summarised in Table 2 and the single grain data are available in online supporting information files. Of the 240 counted grains, two were destroyed during laser analysis, leaving a total of 238 analysed grains. The fission track density ranged from 0.75 to 3.5 × 10^{-6} tracks cm^{-2}. and often showed slight spatial variation on the scale of the grain, implying minor uranium zonation (Figure 1b). The mean track length (MTL – *c* axis projected) is 13.41 ± 0.16 μm (2*s*), with no significant difference between the two mounts (Table S1, Figure S1). The mean Dpar value is 1.58 ± 0.02 μm, and is similar between the two mounts (Table S1, Figure S1). Single grain ages (SGA) range from 162.0 ± 47.5 to 375.6 ± 117.8 Ma while session central ages (CA) range from 238.4 ± 15.1 to 281.6 ± 35.2 Ma (Figure 2). None of the sessions showed large SGA dispersion, with the $p(\chi^2)$ values ranging from 0.12 to 0.99. The most precise (i.e., with the lowest uncertainty) session (No. 9, mapping session) yielded a central age of 251.8 ± 11.7 Ma. Taken together, the 238 grains yield a central age of 254.1 ± 5.1 Ma, with a dispersion of 4.3% and a $p(\chi^2)$ of 0.26. All individual session central ages are consistent with this overall central age.

Single grain U-Pb 207-corrected ages (with an initial $^{207}Pb/^{206}Pb$ ratio of 0.874 – Krestianinov *et al.* 2021) range from 459.4 ± 56.7 to 581.6 ± 40.3 Ma. Taken together the 238 grains yield a lower intercept (regression is anchored at an initial $^{207}Pb/^{206}Pb$ ratio of 0.874) of 523.5 ± 1.7 Ma (MSWD = 0.79, Figure 3a). The lower intercept ages in the Tera-Wasserburg diagram range from 531.6 ± 13.8 to 511.5 ± 7.4 Ma, in accordance with the reference age of 523.51 ± 1.47 Ma (Schoene and

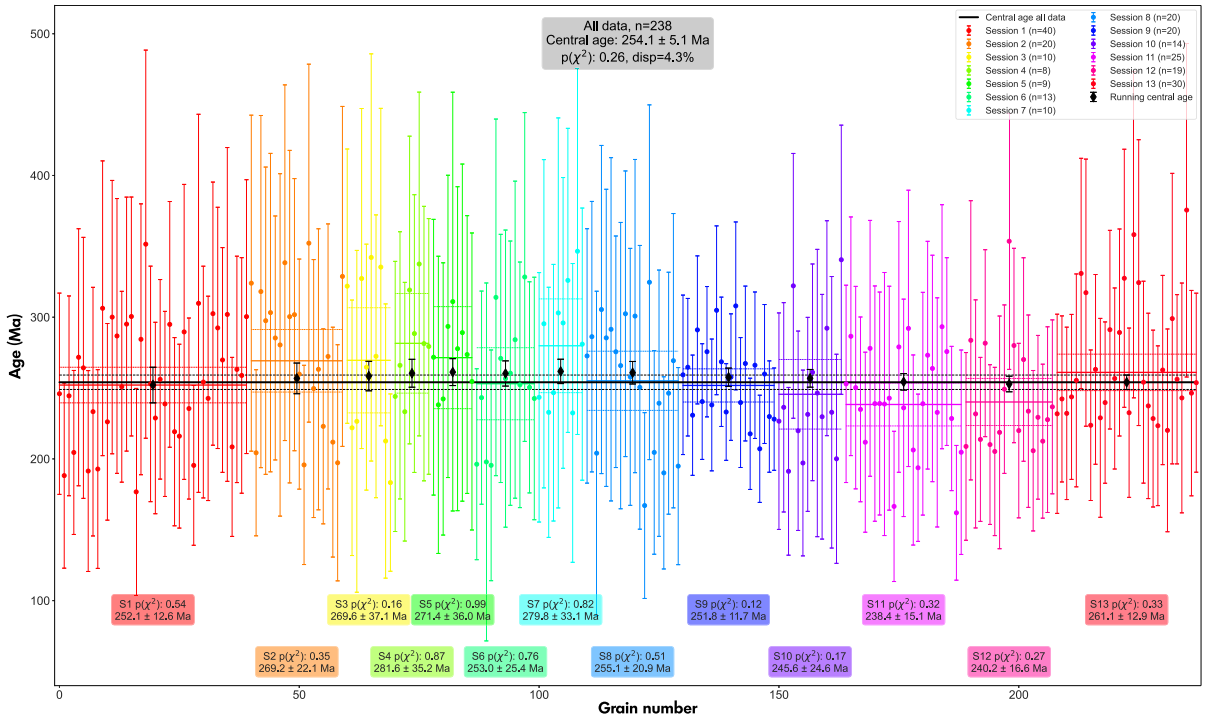

Figure 2. Apatite fission track age plot. Single grain age and uncertainty (2*s*) are colour-coded following session number. For each session the central age and its uncertainty is plotted (thick bar and dashed thin bars, same colour code as single grain data) and are written below the data with $p(\chi^2)$. The number of grains used is indicated in the legend. The overall central age and statistics are also written as title. The running central age (black symbols) shows the variation of the overall central age along the two years of analysis.

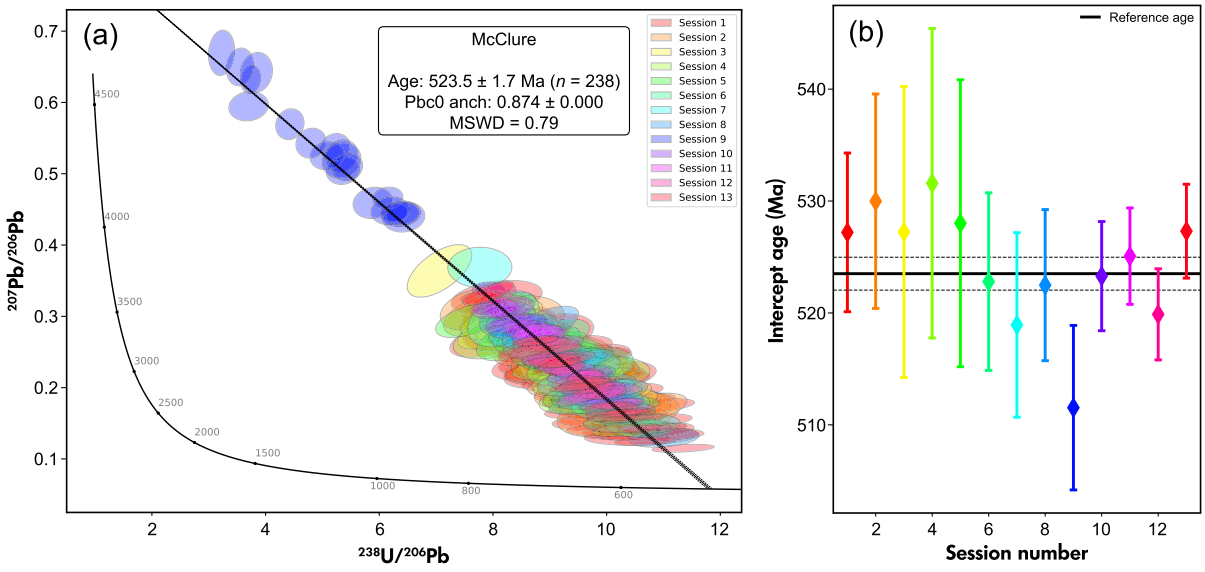

Figure 3. U-Pb data. (a) Tera-Wasserburg diagram for all the analysed grains. The regression is anchored at an initial $^{207}Pb/^{206}Pb$ of 0.88198. Ellipses represent 2*s* and colour coded following session number (see Figure 3b and Figure 2). (b) Concordia lower intercept age and uncertainty (2*s*) for each measurement session. The reference age of Schoene and Bowring (2006) is plotted as a thick black line.

Bowring 2006, Figure 3b) apart for session 9 which is further discussed below.

Trace element mass fractions show some inter-grain variability (Table S1, Figure 4). However, a plot of data normalised to chondrite shows that the pattern of the multi-element spectrum (both abundances and standard deviations) are very similar to that published by Chew *et al.* (2016) (Figure 4a). Additionally our data and those of Chew *et al.* (2016) are similar in a LREE (La–Nd) *versus* Sr/Y plot (Figure 4b) that can be used for discrimination of apatite origin (O'Sullivan *et al.* 2020). The results from MMS apatite are clearly consistent with the overall mafic-ultramafic affinities of the McClure Mountain complex.

Discussion

MMS as a double FT and U-Pb dating validation material

The MMS fission track density is high enough to provide a well-constrained age on a small area and also to identify zoned areas on a grain. The first characteristic is advantageous as it is better to keep the counting area similar to the shape and size of the ablation spot (Cogné and Gallagher 2021). On average, our counted area was approximately 2.5 × 10^{-5} cm^2, which corresponds roughly to a square of 50 µm × 50 µm. With this size and given the track density, about fifteen to twenty grains ensure a central age with less than 10% uncertainty (2*s*). On the other hand, the track density remains low enough to be easily, and thus rapidly, counted.

Our single grain FT age data show good reproducibility for the analyses carried out over two years and thirteen measurement sessions. The SGA dispersion of 4.3% seems reasonable for a natural sample and both individual sessions and all data together show a $p(\chi^2)$ well above 5%, which is consistent with a single age population. All session central ages are in agreement with each other and with the overall central age (254.1 ± 5.1 Ma). The mapping session, following Ansberque *et al.* (2020), was undertaken because of its ability to deal with U zonation on an *X-Y* plan. This allows us to count larger areas, and thus more tracks, which in turn permits a better constrained age. The mapping session yielded a central age of 251.8 ± 11.7 Ma, which is close to the overall central age. The latter is also in agreement with published ages in this area of the Wet Mountains (Kelley and Chapin 2004) and with the published apatite FT age on the McClure Syenite (Olson *et al.* 1977). Therefore, we suggest that a reference apatite FT age 254.1 ± 5.1 Ma can be used for MMS. This age is the result of our thirteen measurement sessions on MM1, but it is possible that different samples from the MMS complex could yield slightly different ages. Although the MMS outcrop is relatively small and the relief is limited to approximately

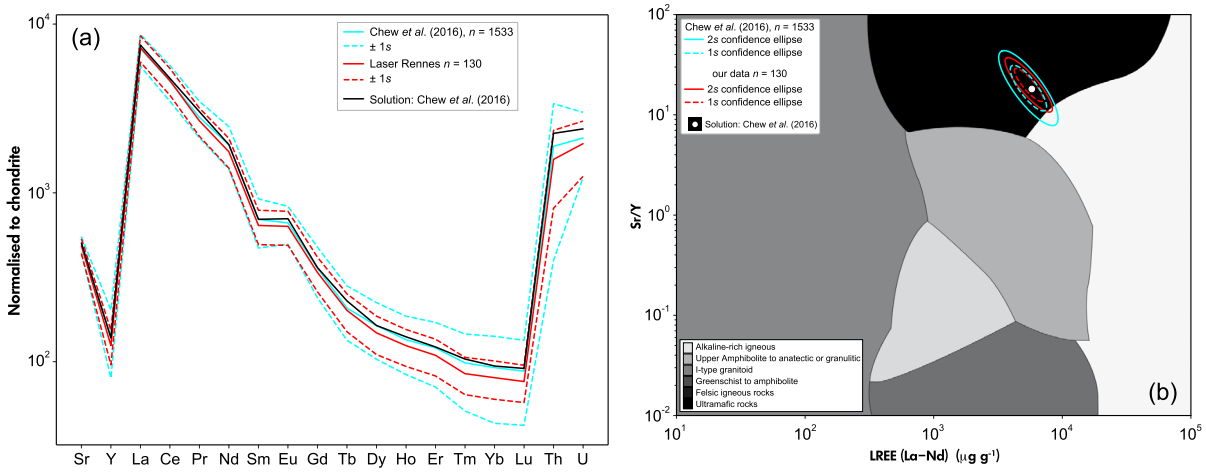

Figure 4. Trace element data. (a) Chondrite-normalised trace element spectrum. Our data are plotted in red, solid line is the mean and dashed lines are the 1 standard deviation (1*s*). Chew *et al.* (2016) laser data are in blue and solution data in black for comparison. (b) LREE versus Sr/Y plot (O'Sullivan *et al.* 2020). Colours are the same as in (a), solid line are the 2*s* ellipses, dashed line the 1*s* ellipses, the white point being solution data of Chew *et al.* (2016). Background field limits are from O'Sullivan *et al.* (2020).

300 m, we also recommend that this age be confirmed by other laboratories and/or FT dating methods.

While MMS could be used for just FT dating, the goal of this study was to propose a secondary reference material for double FT and U-Pb apatite dating. As use of secondary reference materials is common practice for U-Pb, the use of the same material for the both methods is advantageous as it requires only one ablation spot. The MMS also has the advantage of being well characterised for apatite U-Pb age and common lead composition (Schoene and Bowring 2006, Krestianinov *et al.* 2021). Therefore, all our FT dated grains were also dated for U-Pb. The U-Pb results for each session and for all the data together (523.5 ± 1.7 Ma) are in agreement with the reference age (523.51 ± 1.47 Ma, Schoene and Bowring 2006). We therefore argue that MMS is a suitable material for LA-ICP-MS apatite double dating validation. The only supplementary time required for adding FT validation is the track counting time, which thanks to a reasonable track density, is relatively limited in the case of MMS.

We note, however, that session 9 (mapping session) yielded lower U-Pb ratios than usual. There are different possible explanations for this. Firstly, we may have extracted data from the edge of the crystal and possibly included epoxy. Examination of the ^{43}Ca maps show that the areas used for data extraction (the same for FT and U-Pb, mimicking the area of FT counting) were well inside the apatite (a representative example is provided in Figure S2). Secondly, it is possible that we obtained data on part of the grain having lower U-Pb ratios. However, the maps of $^{238}U/^{206}Pb$ are relatively homogeneous, and subsequent spot analyses on the same grains show a more usual $^{238}U/^{206}Pb$ value (i.e., between 8 and 11). We therefore suggest that the difference may come from Pb contamination on the surface. Raster mapping ablates only the very first micrometre or so on the surface of the targeted grains. Then Pb contamination on the surface could have an impact on the measured values. For a Q-ICP-MS, the difference in composition between this contaminant Pb and the common Pb of the grain would remain undetectable. Then the effect of this contamination would be a decrease of the U-Pb ratios, driving the ellipses toward the common Pb end of the Discordia. While this hypothesis could explain the observed data, it would require more work to be tested, which is beyond the scope of this contribution. The intercept age of the session is also slightly younger (2%) than the reference age (511.5 ± 7.4 compared with 523.51 ± 1.47). We do not think that this is linked to the hypothesis of common Pb contamination at the surface of the sample. In any case it does not affect our main conclusion that MMS is suitable for quality control of double AFT and U-Pb dating.

The potential use of MMS for trace element analysis

In addition to obtaining a U-Pb date, the LA-ICP-MS FT dating protocol can also be used for trace element mass fractions (e.g., Cogné *et al.* 2020, Ansberque *et al.* 2021). Data published by Chew *et al.* (2016) for MMS were acquired over a period of 5 years of LA-Q-ICP-MS analysis and more than 1500 individual laser spots. These authors also used solution ICP-MS to assess the accuracy of the LA-Q-ICP-MS element mass fractions, which used NIST SRM 612 as the primary reference material for trace elements. They concluded that for a large series of elements (REE, Mn, V, Y, Sr, Th and U) the LA-ICP-MS results were in agreement with the solution values. However, they noticed that inter-grain variation could be quite important for MMS and at that stage precluded its use as primary reference material for element mass fractions.

We performed determinations for Mn, Sr, Y, REE, Th and U in 130 apatite grains from the MMS. Our measurement results show a good similarity with those of Chew *et al.* (2016), values and ranges being comparable for all the elements (Figure 4). The shapes of the REE-normalised spectra are also very similar. Thus, we argue that despite the inter-grain variability, MMS could also be used as a quality control material for trace element data reduction schemes.

To assess the number of analysed grains required, we merged the two datasets and calculated mean and standard deviation for this whole dataset. We then used a *Python* script to randomly draw a number (n) of analyses. The mean mass fraction for each element was calculated and if this was not in the $\pm 1s$ range of the whole dataset, this draw was defined as 'failed'. This process was repeated 10,000 times with n ranging from 3 to 30. For each n, a percentage of failed draws was calculated. The results show that for more than five analyses, the fail percentage was $< 10\%$ (see Figure S3), $< 5\%$ for more than ten analyses and finally $< 1\%$ with or more twenty-one analyses. Therefore, we assume that analysing ten grains and averaging them should be enough for trace element measurement quality control, but fifteen to twenty analyses would of course be better.

Although most Durango crystals would show lower inter-analysis dispersion, we do not know in advance what the trace element abundances are for a given crystal. In contrast, assuming the MMS sample originated from the car park boulder, we do know the abundances of the various trace elements and their dispersion. Therefore, using MMS has the

advantage of using only one ablation spot for quality control in the case of FT, U-Pb and trace element determinations being measured during the same session. The number of required analysed grains is similar between AFT and trace elements, that is fifteen to twenty.

Conclusions

Results of LA-ICP-MS fission track (FT) dating of MMS apatite over two years of analysis are relatively homogenous in terms of the estimated ages. The track density ensures that the counting part of the dating can readily be performed accurately and with minimal risk of undetected U zonation. As only fifteen to twenty grains are necessary to obtain a well-constrained FT age it can therefore be used easily as a secondary reference material for FT dating. The MMS apatite is already well characterised for U-Pb age and common Pb content, and so it is widely used as secondary reference material for this technique. Therefore, we argue that the MMS is also a suitable material for quality control of apatite double dating using LA-ICP-MS. This would allow the FT community to follow the recommended practice of other geochronological techniques and we advocate that publishing secondary reference material data for LA-ICP-MS FT ages should become common practice.

The trace element data we acquired on the MMS are in very close agreement with the large dataset published by Chew *et al.* (2016). We accept that the inter-grain variation is non-negligible but we think that MMS could also be used as a secondary reference material if trace element measurement is performed at the same time as fission track and U-Pb dating.

Acknowledgements

NC thanks Raymond Donelick for providing MM1 apatite. Paul Sylvester is thanked for editorial handling. Andrew Gleadow and an anonymous reviewer are thanked for their comments that improved the manuscript. The authors declare that they have no conflict of interest.
Scientific editing by Paul J. Sylvester.

Data availability statement

The data that support the findings of this study are available in online supporting information files.

References

Alexander E., Mickelson G. and Lanphere M. (1978) MMhb-1: A new ^{40}Ar-^{39}Ar dating standard. In: **Short Papers of the Fourth International Conference, Geochronology, Cosmochronology, and Isotope Geology. U.S. Geological Survey, 78–701**, 6–8.

Anderson A.J., Hodges K.V. and van Soest M.C. (2017) Empirical constraints on the effects of radiation damage on helium diffusion in zircon. **Geochimica et Cosmochimica Acta, 218**, 308–322.

Anderson A.J., Hodges K.V. and van Soest M.C. (2018) Comment on 'Distinguishing slow cooling versus multiphase cooling and heating in zircon and apatite (U-Th)/He datasets: The case of the McClure Mountain syenite standard' by Weisberg, Metcalf and Flowers. **Chemical Geology, 498**, 150–152.

Ansberque C., Chew D.M. and Drost K. (2021) Apatite fission-track dating by LA-Q-ICP-MS mapping. **Chemical Geology, 560**, 119977.

Boehnke P. and Harrison M.T. (2014) A meta-analysis of geochronologically relevant half-lives: What's the best decay constant? **International Geology Review, 56**, 905–914.

Chew D.M. and Donelick R.A. (2012) Combined apatite fission track and U-Pb dating by LA-ICP-MS and its application in apatite provenance analysis. **Mineralogical Association of Canada Short Course, 42**, 219–247.

Chew D.M., Petrus J.A. and Kamber B.S. (2014a) U-Pb LA-ICP-MS dating using accessory mineral standards with variable common Pb. **Chemical Geology, 363**, 185–199.

Chew D.M., Donelick R.A., Donelick M.B., Kamber B.S. and Stock M. (2014b) Apatite chlorine concentration measurements by LA-ICP-MS. **Geostandards and Geoanalytical Research, 38**, 23–35.

Chew D.M., Babechuk M.G., Cogné N., Mark C., O'Sullivan G.J., Henrichs I.A., Doepke D. and McKenna C.A. (2016) (LA,Q)-ICP-MS trace-element analyses of Durango and McClure Mountain apatite and implications for making natural LA-ICP-MS mineral standards. **Chemical Geology, 435**, 35–48.

Cogné N., Chew D.M., Donelick R.A. and Ansberque C. (2020) LA-ICP-MS apatite fission track dating: A practical zeta-based approach. **Chemical Geology, 531**, 119302.

Cogné N. and Gallagher K. (2021) Some comments on the effect of uranium zonation on fission track dating by LA-ICP-MS. **Chemical Geology, 573**, 120226.

references

De Grave J., Glorie S., Ryabinin A., Zhimulev F., Buslov M.M., Izmer A., Elburg M., Vanhaecke F. and Van den Haute P. (2012)
Late Palaeozoic and Meso-Cenozoic tectonic evolution of the southern Kyrgyz Tien Shan: Constraints from multi-method thermochronology in the Trans-Alai, Turkestan-Alai segment and the southeastern Ferghana Basin. **Journal of Asian Earth Sciences**, **44**, 149–168.

Donelick R.A., O'Sullivan P.B. and Ketcham R.A. (2005)
Apatite fission-track analysis. **Reviews in Mineralogy and Geochemistry**, **58**, 49–94.

Fleischer R.L., Price P.B. and Walker R.M. (1975)
Nuclear tracks in solids: Principles and applications. **University of California Press (Berkeley)**, 605pp.

Flowers R.M., Ketcham R.A., Shuster D.L. and Farley K.A. (2009)
Apatite (U-Th)/He thermochronometry using a radiation damage accumulation and annealing model. **Geochimica et Cosmochimica Acta**, **73**, 2347–2365.

Galbraith R. (2010)
Statistics for LA-ICP-MS fission track dating. **Thermo 2010 – 12th International Conference on thermochronology (Glasgow)**, 175.

Galbraith R.F. and Laslett G.M. (1993)
Statistical models for mixed fission track ages. **Nuclear Tracks and Radiation Measurements**, **21**, 459–470.

Gallagher K. (2012)
Transdimensional inverse thermal history modeling for quantitative thermochronology. **Journal of Geophysical Research**, **117**, B02408.

Gautheron C., Tassan-Got L., Barbarand J. and Pagel M. (2009)
Effect of alpha-damage annealing on apatite (U-Th)/He thermochronology. **Chemical Geology**, **266**, 157-170.

Gautheron C., Pinna-Jamme R., Derycke A., Ahadi F., Sanchez C., Haurine F., Monvoisin G., Barbosa D., Delpech G., Maltese J., Sarda P. and Tassan-Got L. (2021)
Technical note: Analytical protocols and performance for apatite and zircon (U-Th)/He analysis on quadrupole and magnetic sector mass spectrometer systems between 2007 and 2020. **Geochronology**, **3**, 351–370.

Glorie S., Gilbert S.E., Hand M. and Lloyd J.C. (2023)
Calibration methods for laser ablation Rb-Sr geochronology: Comparisons and recommendation based on NIST glass and natural reference materials. **EGUsphere preprint repository.**

Härtel B., Matthews W.A. and Enckelmann E. (2023)
Duluth Complex FC1 apatite and zircon: Reference materials for (U-Th)/He dating? **Geostandards and Geoanalytical Research**, **47**, 669–681.

Hasebe N., Barbarand J., Jarvis K., Carter A. and Hurford A.J. (2004)
Apatite fission-track chronometry using laser ablation ICP-MS. **Chemical Geology**, **207**, 135–145.

Holden N.E. and Hoffman D.C. (2000)
Spontaneous fission half-lives for ground-state nuclide (technical report). **Pure and Applied Chemistry**, **72**, 1525–1562.

Horstwood M.S.A., Košler J., Gehrels G., Jackson S.E., McLean N.M., Paton C., Pearson N.J., Sircombe K., Sylvester P., Vermeesch P., Bowring J.F., Condon D.J. and Schoene B. (2016)
Community-derived standards for LA-ICP-MS U-(Th-) Pb geochronology – Uncertainty propagation, age interpretation and data reporting. **Geostandards and Geoanalytical Research**, **40**, 311–332.

Hurford A.J. (1990)
Standardization of fission track dating calibration: Recommendation by the Fission Track Working Group of the I.U.G.S. Subcommission on Geochronology. **Chemical Geology**, **80**, 171–178.

Hurford A.J. and Green P.F. (1983)
The zeta age calibration of fission-track dating. **Chemical Geology**, **41**, 285–317.

Iwano H., Danhara T., Yuguchi T., Hirata T. and Ogasawara M. (2019)
Duluth complex apatites: Age reference material for LA-ICP-MS-based fission-track dating. **Terra Nova**, **31**, 247–256.

Jochum K.P., Weis U., Stoll B., Kuzmin D., Yang Q., Raczek I., Jacob D.E., Stracke A., Birbaum K., Frick D.A., Günther D. and Enzweiler J. (2011)
Determination of reference values for NIST SRM 610–617 glasses following ISO guidelines. **Geostandards and Geoanalytical Research**, **35**, 397–429.

Kelley S. and Chapin C. (2004)
Denudation history and internal structure of the Front Range and Wet Mountains, Colorado, based on apatite fission track thermochronology. **New Mexico Bureau of Geology and Mineral Resources Bulletin**, **160**, 41–78.

Klemme S., John T., Wessels M., Kusebauch C., Berndt J., Rohrbach A. and Schmid-Beurmann P. (2013)
Synthesis of trace element bearing single crystals of chlor-apatite ($Ca_5(PO_4)_3Cl$) using the flux growth method. **Chemistry Central Journal**, **7**, 56.

Krestianinov E., Amelin Y., Neymark L.A. and Aleinikoff J.N. (2021)
U-Pb systematics of uranium-rich apatite from Adirondacks: Inferences about regional geological and geochemical evolution, and evaluation of apatite reference materials for *in situ* dating. **Chemical Geology**, **581**, 120417.

Ludwig K.R. (1980)
Calculation of uncertainties of U-Pb isotope data. **Earth and Planetary Science Letters**, **46**, 212–220.

McDowell F.W., McIntosh W.C. and Farley K.A. (2005)
A precise ^{40}Ar-^{39}Ar reference age for the Durango apatite (U-Th)/He and fission-track dating standard. **Chemical Geology**, **214**, 249–263.

Naeser C.W. (1967)
The use of apatite and sphene for fission track age determinations. **Geological Society of America Bulletin**, **78**, 1523–1526.

references

Olson J., Marvin R., Parker R. and Mehnert H. (1977)
Age and tectonic setting of Lower Paleozoic alkalic and mafic rocks, carbonatites, and thorium veins in south-central Colorado. **Journal of Research of the U.S. Geological Survey, 5**, 673–687.

O'Sullivan G.O., Chew D., Kenny G., Henrichs I. and Mulligan D. (2020)
The trace element composition of apatite and its application to detrital provenance studies. **Earth-Science Reviews, 201**, 103044.

Paces J.B. and Miller J.D. (1993)
Precise U-Pb ages of Duluth Complex and related mafic intrusions, northeastern Minnesota: Geochronological insights to physical, petrogenetic, paleomagnetic, and tectonomagmatic processes associated with the 1.1 Ga Midcontinent Rift system. **Journal of Geophysical Research, 98**, 13997–14013.

Paton C., Hellstrom J., Paul B., Woodhead J. and Hergt J. (2011)
Iolite: Freeware for the visualisation and processing of mass spectrometric data. **Journal of Analytical Atomic Spectrometry, 26**, 2508–2518.

Price P. and Walker R. (1962)
Observation of fossil particle tracks in natural micas. **Nature, 196**, 732–734.

Samson S. and Alexander Jr. E.C. (1987)
Calibration of the interlaboratory ^{40}Ar-^{39}Ar dating standard, MMhb-1. **Chemical Geology (Isotope Geoscience Section), 66**, 27–34.

Schoene B. and Bowring S.A. (2006)
U–Pb systematics of the McClure Mountain syenite: Thermochronological constraints on the age of the $^{40}Ar/^{39}Ar$ standard MMhb. **Contributions to Mineralogy and Petrology, 151**, 615–630.

Soares C., Guedes S., Hadler J., Mertz-Kraus R., Zack T. and Iunes P. (2014)
Novel calibration for LA-ICP-MS-based fission-track thermochronology. **Physics and Chemistry of Minerals, 41**, 65–73.

Shawe D.R. and Parker R.L. (1967)
Mafic-ultramafic layered intrusion at Iron Mountain, Fremont County, Colorado. **United States Geological Survey Bulletin, 1251-A**, A1–A20.

Spell T. and McDougall I. (2003)
Characterization and calibration of $^{40}Ar/^{39}Ar$ dating standards. **Chemical Geology, 198**, 189–211.

Thomson S.N., Gehrels G.E., Ruiz J. and Buchwaldt R. (2012)
Routine low-damage apatite U-Pb dating using laser ablation-multicollector-ICP-MS. **Geochemistry, Geophysics, Geosystems**, 13.

Vermeesch P. (2017)
Statistics for LA-ICP-MS based fission track dating. **Chemical Geology, 456**, 19–27.

Vermeesch P. (2019)
Statistics for fission-track thermochronology. **In: Malusà M.G. and Fitzgerald P.G. (eds), Fission-track thermochronology and its application to geology. Springer (Berlin)**, 109–122.

Weisberg W.R., Metcalf J.R. and Flowers R.M. (2018)
Distinguishing slow cooling versus multiphase cooling and heating in zircon and apatite (U-Th)/He datasets: The case of the McClure Mountain syenite standard. **Chemical Geology, 485**, 90–99.

Woodhead J., Hellstrom J., Hergt J., Greig A. and Maas R. (2007)
Isotopic and elemental imaging of geological materials by laser ablation-inductively coupled plasma-mass spectrometry. **Geostandards and Geoanalytical Research, 31**, 331–343.

York D., Evensen N.M., Lopez Martinez M. and De Basabe Delgado J. (2004)
Unified equations for the slope, intercept, and standard errors of the best straight line. **American Journal of Physics, 72**, 367–375.

Supporting information

The following supporting information may be found in the online version of this article:

Figure S1. Dpar and track length histograms for the two sessions in which they were measured.

Figure S2. Isotopic maps of grain 10 of the McClure mount 2. The black line represents the area of data extraction that mimics the area of track counting. (a) ^{43}Ca map, showing that the area is well inside the grain and (b) Final $^{206}Pb/^{238}U$ showing a good homogeneity at the scale of the grain. See text for explanation.

Figure S3. Plot of results of a random draw of trace element abundances. The *y*-axis indicates the percentage of the random draw that failed over 10,000 iterations for a number of analyses randomly picked indicated on the *x*-axis. See text for explanation.

Table S1. Individual grain measurement results. Track length and Dpar data are also reported.

This material is available from: http://onlinelibrary.wiley.com/doi/10.1111/ggr.12545/abstract (This link will take you to the article abstract).